Biochemical and Biophysical Research Communications 458 (2015) 294–299

Contents lists available at ScienceDirect

Biochemical and Biophysical Research Communications

journal homepage: www.elsevier.com/locate/ybbrc

Identification and functional characterization of voltage-gated sodium channels in lymphocytes

Weifeng Huang [a], Chunjing Lu [b], Yong Wu [a], Shou Ouyang [c], Yuanzhong Chen [a, *]

[a] Fujian Institute of Hematology, Fujian Medical University Union Hospital, Fuzhou 350004, PR China
[b] Department of Blood Transfusion, Maternal and Child Health Hospital of Xiamen, Xiamen 361003, PR China
[c] Xiamen Medical Research Institute, Xiamen 361008, PR China

ARTICLE INFO

Article history:
Received 14 January 2015
Available online 31 January 2015

Keywords:
Lymphocytes
Voltage-gated sodium channel
Invasion

ABSTRACT

A variety of ion channels has been discovered in lymphocytes. RT-PCR and real-time PCR analysis revealed that ALL (acute lymphocytic leukemia) cell lines and human peripheral blood mononuclear cells mainly expressed TTX (tetrodotoxin)-sensitive voltage-gated sodium channels (VGSCs). Expression of VGSC protein was confirmed by western blots and Immunofluorescence. Whole-cell patch-clamp recordings showed that a sub-population (20%) of MOLT-4 cells expressed functional VGSCs, which were TTX-sensitive. Importantly, 2 μM TTX decreased the invasion of Jurkat and MOLT-4 cells ~90%. These results indicate that the activity of VGSCs could represent a novel mechanism potentiating the invasive capacity of these cells.

1. Introduction

A variety of ion channels has been discovered in lymphocytes, including voltage-gated potassium channels ($K_V1.3$) [1–3], calcium-activated potassium channels (K_{Ca}) [4,5], calcium release-activated calcium channels (CRAC) [6,7], and swelling-activated chloride channels (Cl_{swell}) [8]. Expression levels of ion channels in human T cells vary dramatically during thymic development, activation, and differentiation to effector cells [9].

To mount an effective immune response, T and B lymphocytes must migrate into tissue, which depends on the regulated trafficking of lymphocytes [10]. This 'homing' process eventually leads to the recruitment of immune effector cells to sites of antigenic or microbial invasion. Circulating lymphocytes are round, 'non-motile' cells, which redistribute their cytoskeletal elements and organelles to acquire a constantly changing shape and polarized morphology during inflammatory response [11]. However, the mechanism(s) underlying this response is not yet clear. There is increasing evidence suggesting that cancer metastasis is controlled by voltage-gated sodium channel (VGSC) activity [12–18]. Accordingly, the specific VGSC blocker TTX suppresses a variety of metastatic cell behaviors in vitro [13–18]. Interestingly, parallels have been drawn between lymphocyte trafficking and cancer metastasis [19,20]. Therefore, investigating the expression and function of VGSC in lymphocytes is necessary for better understanding the roles of lymphocytes during immune responses.

Cells of the immune system traditionally have been categorized as 'electrically inexcitable'. However, after activation, they pose some electrophysiological properties of "electrically excitable cells" owning to changes in expression patterns of ion channels and intracellular Ca^{2+} mobilization. Human T lymphocytes express VGSCs under tight control [15], but their molecular identity and functional roles in these cells are not yet well known. The VGSC consists of a major pore-forming α-subunit (250–260 kDa) and a variable number of auxiliary β-subunits (30–40 kDa) [21]. The mammalian VGSCα gene family contains at least 9 functional members ($Na_v1.1$-$Na_v1.9$, coded by genes SCN1A-SCN11A) identified to date [21]. Each isoform exhibits a specific sensitivity to the selective blocker TTX and two groups of VGSC isoforms are described, the TTX-sensitive (TTX-S: $Na_v1.1$, $Na_v1.2$, $Na_v1.3$, $Na_v1.4$, $Na_v1.6$ and $Na_v1.7$) and the TTX-resistant (TTX-R: $Na_v1.5$, $Na_v1.8$ and $Na_v1.9$) sodium channels, which are blocked by TTX at nM and μM levels, respectively.

Although VGSCs are already known to occur in lymphocytes, their molecular identity and isoforms are not yet well known. In addition, there are little reports about the functional roles of VGSCs in lymphocytes. The main aims of the present study were 2-fold: (i) to investigate the molecular identity of the VGSCα in lymphocyte

* Corresponding author.
E-mail address: 58301694@qq.com (Y. Chen).

http://dx.doi.org/10.1016/j.bbrc.2015.01.103
0006-291X/

cells; and (ii) to explore the role of VGSCs in the lymphocyte invasion. In the present investigation, we carefully identified the expression isoforms of VGSC in lymphocytes using RT-PCR, qPCR, western blots, Immunofluorescence (IF) and patch-clamp recordings. Our results suggest a novel mechanism potentiating the invasive capacity of lymphocytes.

2. Materials and methods

2.1. Cell culture

The human lymphocyte cell leukemia line MOLT-4, Jurkat and Ball were obtained from American Type Culture Collection (ATCC; Rockville, MD, USA) maintained in RPMI 1640 medium supplemented with 10% heat-inactivated fetal bovine serum (Gibco by Life Technologies, Carlsbad, CA, USA), 1% pen/strep (MP Biomedicals, Solon, OH, USA) and 2 mM L-glutamine at 37 °C in 95% air/5% CO_2 with 95% humidity. Culture media was replaced every 2–3 days.

2.2. Isolation of human peripheral blood mononuclear cells

Whole blood (5–10 ml) was collected from healthy human male and female donors (n = 9 each), according to The Code of Ethics of the World Medical Association. Mononuclear cells were isolated with human lymphocyte separation medium (Tbdscience, Tianjin, China) according to manufacturer's instructions. Briefly, human peripheral blood mononuclear cells (PBMCs) were separated by centrifugation at 900 × g for 30 min at 18–20 °C over a Ficoll–Paque PLUS gradient. The resulting PBMC layer was washed twice with nuclease-free 0.9% NaCl solution and prepared for RNA isolation.

2.3. Reverse transcriptase-polymerase chain reaction (RT-PCR)

Total cellular RNA was isolated from exponentially growing cells and human PBMCs using RNAsimple Total RNA Kit (TIANGEN Biotech, Beijing, China). Messenger RNA was reverse-transcribed (RT) to cDNA using oligo$(dT)_{15}$ primers and GoScript reverse transcriptase (Promega, Madison, WI, USA). The cDNA product was used as a template for subsequent PCR amplifications for VGSCα subunit, using sequence-specific primers. Primer sequences and product sizes are summarized in Table 1. The temperature profile was 2 min at 94 °C followed by amplification for 38 cycles which consisted of 30 s at 94 °C, 30 s at 60 °C, and 1 min at 72 °C and a final extension for 7 min at 72 °C. PCR analysis was repeated at least three times with the same samples to confirm reproducibility of the results.

2.4. Quantitative PCR

Total RNA 1 μg was used to generate cDNA with GoScript reverse transcriptase as above. A 1-μl aliquot of each synthesized cDNA was analyzed by Quantitative Real-Time PCR (CFX96 Real-Time System, Bio-Rad, Singapore) using SYBR Green PCR Master Mix (Takara, Dalian, China) according to manufacturer's protocols and message level was determined using the $\triangle C_t$ method. Samples were assayed in triplicate for each gene, and the mean expression was used during subsequent analysis. QRT-PCR was carried out under the following reaction conditions: stage 1, 95 °C for 30 s (Rep 1); stage 2, 95 °C for 5 s then 60 °C for 1 min (Reps 40).

2.5. Western blot analysis

Cells were washed twice with ice-cold phosphate-buffered saline (PBS) and then resuspended in an RIPA lysis buffer (BOSTER, Wuhan, China) supplemented with 1% PMSF (Beyotime, Nantong, China). The samples were kept on ice for 1 h and then sonicated for 15 s. They were then centrifuged at 13,000 × g for 10 min at 4 °C. Total protein concentrations were determined in triplicate by BCA protein assay kit (Beyotime, Nantong, China). Supernatants were denatured by heat shock at 95 °C for 5 min in SDS buffer before being loaded at a total protein concentration of 100 μg per lane and run on a 4–15% gradient gel (Willget, Shanghai, China). Protein samples were then transferred to PVDF membranes (Millipore, Bedford, MA, USA). Non-specific binding was blocked by incubation with TBST (10 mM Tris–HCl, 150 mM NaCl, 0.1% Tween-20, pH 7.4) plus 5% non-fat milk for 1 h at room temperature. Then the membrane was incubated overnight at 4 °C with gentle shaking with a pan-specific Na_v rabbit polyclonal antibody (1:200 dilution, Alomone Labs, Israel). Immunoblots were developed with a goat anti-rabbit horseradish peroxidase-conjugated secondary antibody (1:10,000; Santa Cruz Biotechnology, Santa Cruz, CA, USA) incubated for 1 h at room temperature. Immunoblots were visualized with the ECL immunodetection system (Advansta, Menlo Park, CA, USA).

2.6. Immunofluorescence

Growth medium was removed and rinsed with PBS. Cells were fixed in 4% paraformaldehyde for 20 min, rinsed, then were plated on poly-L-lysine coated glass coverslips for 2 h. Then the cells were permeabilized with 0.5% Triton-X100-PBS for 10 min. After blocking with 5% BSA, the cells were incubated with a pan-specific Na_v rabbit polyclonal antibody (1:50 dilution, Alomone Labs) overnight at 4 °C. The cells were then rinsed and incubated with goat anti-rabbit IgG (Santa Cruz Biotechnology, Santa Cruz, CA, USA) conjugated to Oregon green (FITC) at a 1:100 dilution for 1 h in dark. The cells were also counterstained with the nuclear stain, DAPI. Then cells were rinsed and subjected to microscopy. The glass coverslips were examined under a Nikon Eclipse Ti–U microscope (Nikon, Tokyo, Japan) equipped with a 20× objective.

2.7. Whole-cell patch-clamp recording

Cells were grown on poly-L-lysine-coated glass coverslips. The electrophysiological techniques used have been described in detail previously [22]. For Na^+ current recordings, low-pass filtered at

Table 1
Oligonucleotides used to amplify transcripts of VGSCα subunits.

Gene name	Gene product	Forward primer 5′ → 3′	Reverse primer 5′ → 3′	Predicted size (bp)
SCN1A	$Na_v1.1$	TTCATGGCTTCCAATCCTTC	TAGCCCCACCTTTGATTTTG	178
SCN2A	$Na_v1.2$	GCCAGCTTATCAATCCCAAA	TCTTCTGCAATGCGTTGTTC	192
SCN3A	$Na_v1.3$	CAAAGGGAAGATCTGGTGGA	AAAGGCCAATGCACCACTAC	115
SCN4A	$Na_v1.4$	TCAACAACCCCTACCTGACC	ACGGACGAGTTCCCATCATA	148
SCN5A	$Na_v1.5$	CACGCGTTCACTTTCCTTC	CATCAGCCAGCTTCTTCACA	208
SCN8A	$Na_v1.6$	CGCCTTATGACCCAGGACTA	GTGCCTCTTCCTGTTGCTTC	247
SCN9A	$Na_v1.7$	GGCTCCTTGTTTTCTGCAAG	TGGCTTGGCTGATGTTACTG	196
SCN10A	$Na_v1.8$	ACCTGGTGGTGCTTAACCTG	TGCTGAAGAAGCTGCAAAGA	168
SCN11A	$Na_v1.9$	CTGTGGTCCTGGTCATTGTG	TGCATTCGCTTCTTGCATAC	233

10 kHz and data sampled at 50 kHz. The cells were superfused with bath solution containing (in mmol/L): 5 HEPES, 130 NaCl, 10 CsCl, 1.8 $CaCl_2$, 1 $MgCl_2$, 10 glucose, 0.5 $CdCl_2$, pH 7.4 adjusted with NaOH. Equimolar choline chloride was used as the substitute for NaCl in Na^+-free experiments. The resistance of pipettes ranged 3–5 MΩ when filled with internal solution containing (in mmol/L): 10 HEPES, 120 CsCl, 10 NaCl, 1 $MgCl_2$, 10 TEA-Cl, 10 EGTA, 5 Na_2ATP, 1.2 Creatine phosphate, adjusted to pH 7.2 with CsOH. Liquid junction potential was not compensated. Following whole cell access, the cells were held at −100 mV with test pulses ranging from −60 mV to +40 mV with 10 mV increments.

2.8. Cell growth assay

To determine cell survival and proliferation, cell growth was quantified using the CellTiter 96 AQ One Solution Cell Proliferation Assay Kit (Promega, Madison, WI, USA). Cells were plated in 96-well culture plates at a density of $1–2 \times 10^4$ cells/well in 100 μL of cell culture media. Cells were treated with different concentrations of TTX (Sigma–Aldrich, St. Louis, MO, USA). After drug exposure, 20 μL of CellTiter 96 AQ One Solution Reagent was added to each well and allowed to incubate for 2 h at 37 °C. The quantity of formazan product formed, which is directly proportional to the number of viable cells, was measured on a Multi-Mode Microplate Reader (MD SpectraMax M3, CA, USA) at 490 nm wavelength using a reference filter at 650 nm wavelength. Viability assays were performed at least three times in independent experiments, using triplicate measurements in each.

2.9. Migration and in vitro invasion assay

Migration was analyzed in 24-well plates receiving 8 μm Transwell pore filters (Corning, NY, USA). The upper compartment was seeded with 5×10^5 cells/ml cells in FBS-free culture medium. The lower compartment was filled with their culture medium supplemented with 10% FBS, as a chemoattractant. In vitro invasion was assessed using the same inserts and the same protocol as above but with the membrane covered with Matrigel basement membrane matrix (BD Biosciences, Bedford MA, USA), an extracellular mimicking matrix. Migration and invasion assays were performed both in the presence and absence of 2 μM TTX and were repeated three times. Invaded cells were quantified after 7 h by either (i) counting 20 fields of view (at 20× objective; under a Nikon Eclipse Ti–U microscope, Nikon, Tokyo, Japan) or (ii) counting cells using a flow cytometer (BD Accuri C6, Ann Arbor, MI, USA).

2.10. Data analysis

All quantitative data are presented as means ± SEM. Statistical significance was determined by Student's t-test. Results were considered significant at $P < 0.05$.

3. Results

3.1. Molecular identity of VGSC isoforms in ALL cell lines and human PBMCs

The gene expression pattern for all isoforms of VGSC was investigated in ALL cell lines and human PBMCs by RT-PCR and real-time PCR. All cell lines and human PBMCs expressed numerous mRNAs for α subunits of VGSC. $Na_v1.3$, $Na_v1.6$, and $Na_v1.7$ mRNA (TTX-S) were the main isoforms (Fig. 1 and Table 2). No specific pattern of mRNA expression could be distinguished between PBMCs and ALL cell lines (Table 2). Furthermore, the presence of the VGSC protein was studied in Jurkat and MOLT-4 T cell lines. Western blots using a pan-specific Na_v channel antibody detected a band of approximately 250 kDa (Fig. 2A). In addition, the addressing of the protein to the membrane was evaluated in both cells using immunolabeling with a pan-specific Na_v antibody. As shown in Fig. 2B, VGSC protein was clearly located at the membrane of some MOLT-4 and Jurkat cells.

3.2. Electrophysiology

MOLT-4 cells showed a mean resting potential of −30.5 ± 1.8 mV (n = 12) and membrane capacitance of 14.5 ± 0.7 pF (n = 15). In 20% (n = 10/51) of recorded cells, membrane depolarization evoked an inward current that reached a peak within a few milliseconds and then inactivated completely (Fig. 3A). Removal of external sodium ions ("Na^+-free solution") induced the total disappearance of the fast inward current (Fig. 3C). In addition, application of the specific inhibitor TTX (2 μM) completely blocked this inward current without unmasking any other voltage-gated inward current (Fig. 3D), which is consistent with the properties of TTX-S Na^+ channels. Fig. 3B showed the Na^+ current–voltage relationships for MOLT-4 T cell line. These currents activated above −30 mV, reaching a peak at around 0 mV. Together, these results demonstrate that TTX-S VGSCs contribute to the recording inward current in MOLT-4 cells.

3.3. Involvement of VGSCs in the cell proliferation, migration and invasion of human T cell leukemia lines

To determine possible functional consequences of VGSC activity, cell proliferation, migration and invasion assays were performed. As shown in Fig. 4A and B, cell proliferation and migration were not sensitive to the presence of TTX in the culture medium in MOLT-4 and Jurkat T cell lines. Interestingly, in vitro invasion of the both cells was sensitive to TTX. Indeed, 2 μM TTX reduced cell invasiveness by ~90% ($P < 0.001$; n = 3; Fig. 4C).

4. Discussion

In the present investigation, we show that ALL cell lines and human PBMCs mainly express TTX-S VGSCs that potentiate the cells' invasiveness. RT-PCR and real-time PCR analysis of the mRNAs revealed the expression of a multiplicity of VGSC encoding α subunits, with $Na_v1.3$, $Na_v1.6$, and $Na_v1.7$ being the most possible candidates contributing to Na^+ current in these cells. In contrast, TTX-R VGSCα, $Na_v1.5$ was expressed at low level in ALL cell lines and human PBMCs. These results are inconsistent with Fraser et al. report [15], which could be due to the differences in experimental

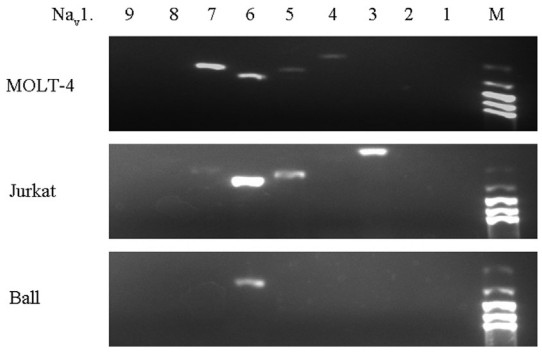

Fig. 1. Expression of VGSCα subunit identified by RT-PCR amplification in MOLT-4, Jurkat and Ball cell lines. M, DNA marker.

Table 2
Q-RT-PCR detected VGSCα subunits expression on MOLT-4, Jurkat, Ball cell lines and PBMCs ($\triangle C_t$).

Cell types	Nav1.1	Nav1.2	Nav1.3	Nav1.4	Nav1.5	Nav1.6	Nav1.7	Nav1.8	Nav1.9
MOLT-4	NA, CT > 40	NA, CT > 40	NA, CT > 40	13.49 ± 0.12	13.88 ± 0.15	13.02 ± 0.16	10.71 ± 0.13	NA, CT > 40	16.89 ± 0.18
Jurkat	NA, CT > 40	NA, CT > 40	8.15 ± 0.17	NA, CT > 40	13.7 ± 0.20	9.63 ± 0.23	13.26 ± 0.19	NA, CT > 40	14.71 ± 0.12
Ball	NA, CT > 40	NA, CT > 40	NA, CT > 40	NA, CT > 40	18.99 ± 0.24	16.74 ± 0.15	20.4 ± 0.23	NA, CT > 40	18.11 ± 0.19
PBMCs	NA, CT > 40	NA, CT > 40	NA, CT > 40	NA, CT > 40	13.50 ± 0.26	10.54 ± 0.11	8.78 ± 0.21	NA, CT > 40	16.12 ± 0.23

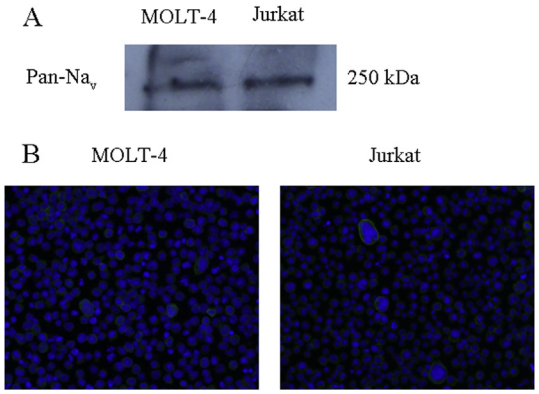

Fig. 2. Expression of VGSCα subunit in Jurkat and MOLT-4 T cell lines. (A) Western blot experiments showing the expression of Na_v α-subunits in cell lines. (B) Cellular localization of pan-Na_v channels in Jurkat and MOLT-4 T cells using Immunofluorescence.

methods between different research groups and highlight the need for cell line authentication.

In the present study, the patch-clamp recording results demonstrated that the inward current in MOLT-4 cells activated at −30 mV, with peak current at 0 mV, in agreement with Annunziato and Diaz reports of recording Na^+ current [17,18]. The electrophysiological properties of recording Na^+ current correspond with $Na_v1.7$ being the most subunit in MOLT-4 cells [17]. Furthermore, 2 μM TTX could block the inward current completely. Taken together, the data suggest that the inward current recorded mainly attributed to TTX-S VGSCs, Nav1.7 in MOLT-4 cells. In addition, current-clamp recordings showed that the mean resting potential was −30.5 ± 1.8 mV in MOLT-4 cells, which is consistent with the occurrence of VGSC window current [17], providing the pattern of Na^+ signaling required for cell metastasis. Interestingly, since we detected functional VGSCs in only 20% of MOLT-4 cells, VGSC expression would appear to be under tight control during lymphocyte activation.

The invasion assays demonstrated that TTX significantly blocked invasiveness of the Jurkat and MOLT-4 cells by about 90%. As TTX is a highly specific blocker of VGSCs, it would suggest that VGSC

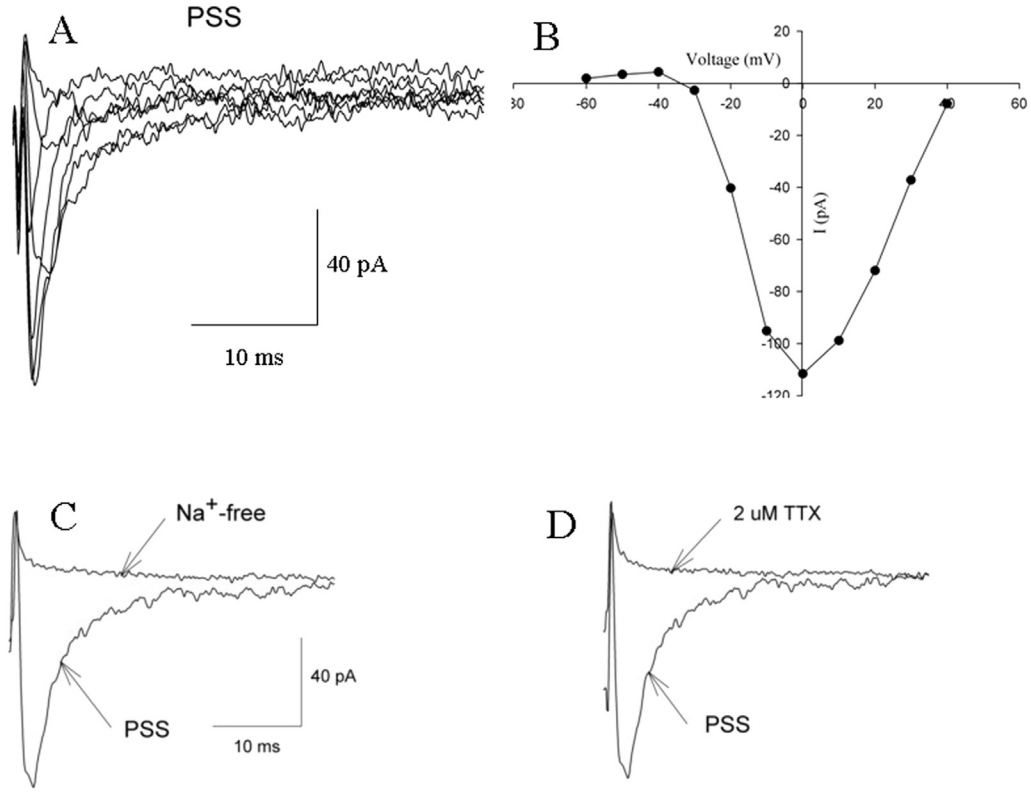

Fig. 3. Electrophysiological recordings from MOLT-4 T cells. (A) Traces showing typical recording of the Na^+ current triggered from a holding potential of −100 mV to 30 ms-long depolarizing steps at −60 to +40 mV (10 mV increments) with an interpulse interval of 2 s. (B) A plot of the current–voltage relationship for the Na^+ current recorded as detailed in (A). (C) and (D) Ionic characterization of the fast inward current recorded in the MOLT-4 T cell line. (C) In presence of PSS, containing 130 mM Na^+, the current triggered by a depolarizing step of 0 mV from a holding potential of −100 mV was recorded, while when external Na^+ was replaced by equimolar choline chloride, it disappeared. (D) The effect of 2 μM TTX on the inward current.

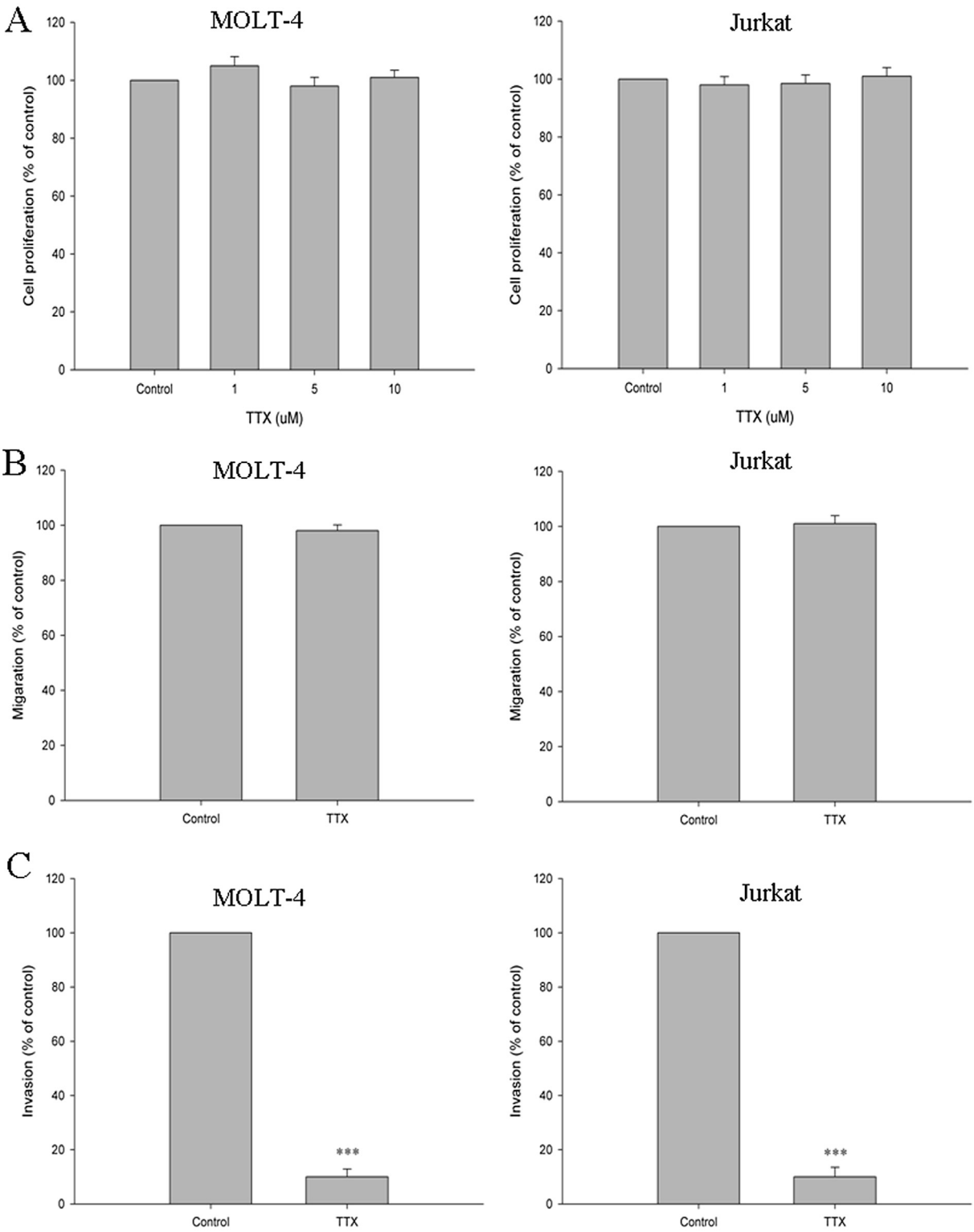

Fig. 4. Effect of VGSC in the proliferation, migration and invasion of human T cell leukemia lines. (A) Relative effect of the TTX on cell proliferation at different concentrations after 48 h incubation. (B) and (C) Effect of 2 μM TTX on cell migration and invasion as compared to control without TTX. Data are presented normalized to control values of 100% and are the mean ± SEM of three independent experimental repeats. $^{***}P < 0.001$ versus control.

activity would normally potentiate T cell invasion. However, the precise mechanism(s) underlying which the VGSCs could regulate cellular invasiveness is not yet known. Since TTX suppressed invasion but not migration, it might be inferred that the activity of VGSCs controlled more secretion of yet non-identified proteases which were necessary to digest the extracellular matrix. For example, I_{Na} through VGSC was shown to acidify the'perimembrane' pH, thus enhancing the proteolytic activity of secreted cysteine cathepsins towards the surrounding extracellular matrix, ultimately resulting in the invasive phenotype of MDA-MB-231

breast cancer cells [23]. In addition, the β subunit is necessary for cytoskeletal linkage and could also function as a cell adhesion molecule mediating interaction with the ECM, cell migration and aggregation [24,25].

In conclusion, our results demonstrate that ALL cell lines express a functional TTX-S VGSC, which mediates the invasiveness of these cells. As human PBMCs also express VGSCs, it is tempting to speculate that VGSCs may play an important role in the invasive properties of normal human T lymphocytes necessary to their intra-/extra-vasation and inflammatory response.

Conflict of interest

The authors have no conflicts of interest to declare.

Acknowledgments

This project was supported by the Chinese National Key Program of Clinical Science (Hematology), the Fujian Provincial Key Laboratory on Hematology Program (No. 2009J1004), Natural Science Funding of Fujian Province (No. 2013D009), the Department of Health of Fujian Province (No. 2014-CXB-48), the Key Sci-Tech Special Project of Fujian (No. 09ZD001), Scientific Research Foundation for the Young Scholars of Fujian Province (No. 2010-2-112), and Project of Xiamen Municipal Science and Technology Commission (No. 3502Z20134044).

References

[1] K.G. Chandy, C.B. Williams, R.H. Spencer, B.A. Aguilar, S. Ghanshani, B.L. Tempel, G.A. Gutman, A family of three mouse potassium channel genes with intronless coding regions, Science 247 (1990) 973–975.
[2] S. Grissmer, B. Dethlefs, J.J. Wasmuth, A.L. Goldin, G.A. Gutman, M.D. Cahalan, K.G. Chandy, Expression and chromosomal localization of a lymphocyte K+ channel gene, Proc. Natl. Acad. Sci. U S A 87 (1990) 9411–9415.
[3] Y.C. Cai, P.B. Osborne, R.A. North, D.C. Dooley, J. Douglass, Characterization and functional expression of genomic DNA encoding the human lymphocyte type n potassium channel, DNA Cell. Biol. 11 (1992) 163–172.
[4] R. Desai, A. Peretz, H. Idelson, P. Lazarovici, B. Attali, Ca2+-activated K+ channels in human leukemic Jurkat T cells. Molecular cloning, biochemical and functional characterization, J. Biol. Chem. 275 (2000) 39954–39963.
[5] S. Grissmer, A.N. Nguyen, M.D. Cahalan, Calcium-activated potassium channels in resting and activated human T lymphocytes. Expression levels, calcium dependence, ion selectivity, and pharmacology, J. Gen. Physiol. 102 (1993) 601–630.
[6] R.S. Lewis, M.D. Cahalan, Mitogen-induced oscillations of cytosolic Ca2+ and transmembrane Ca2+ current in human leukemic T cells, Cell. Regul. 1 (1989) 99–112.
[7] M. Hoth, R. Penner, Calcium release-activated calcium current in rat mast cells, J. Physiol. 465 (1993) 359–386.
[8] R.S. Lewis, P.E. Ross, M.D. Cahalan, Chloride channels activated by osmotic stress in T lymphocytes, J. Gen. Physiol. 101 (1993) 801–826.
[9] M.D. Cahalan, H. Wulff, K.G. Chandy, Molecular properties and physiological roles of ion channels in the immune system, J. Clin. Immunol. 21 (2001) 235–252.
[10] E.C. Butcher, L.J. Picker, Lymphocyte homing and homeostasis, Science 272 (1996) 60–66.
[11] M.V. Parsey, G.K. Lewis, Actin polymerization and pseudopod reorganization accompany anti-CD3-induced growth arrest in Jurkat T cells, J. Immunol. 151 (1993) 1881–1893.
[12] S.P. Fraser, J.K. Diss, A.M. Chioni, et al., Voltage-gated sodium channel expression and potentiation of human breast cancer metastasis, Clin. Cancer Res. 11 (2005) 5381–5389.
[13] W.J. Brackenbury, A.M. Chioni, J.K. Diss, M.B. Djamgoz, The neonatal splice variant of $Na_v1.5$ potentiates in vitro invasive behaviour of MDA-MB-231 human breast cancer cells, Breast Cancer Res. Treat. 101 (2007) 149–160.
[14] M.E. Laniado, E.N. Lalani, S.P. Fraser, J.A. Grimes, G. Bhangal, M.B. Djamgoz, P.D. Abel, Expression and functional analysis of voltage-activated Na+ channels in human prostate cancer cell lines and their contribution to invasion in vitro, Am. J. Pathol. 150 (1997) 1213–1221.
[15] S.P. Fraser, J.K. Diss, L.J. Lloyd, F. Pani, A.M. Chioni, A.J. George, M.B. Djamgoz, T-lymphocyte invasiveness: control by voltage-gated Na+ channel activity, FEBS. Lett. 569 (2004) 191–194.
[16] S. Roger, J. Rollin, A. Barascu, P. Besson, P.I. Raynal, S. Iochmann, M. Lei, P. Bougnoux, Y. Gruel, J.Y. Le Guennec, Voltage-gated sodium channels potentiate the invasive capacities of human non-small-cell lung cancer cell lines, Int. J. Biochem. Cell. Biol. 39 (2007) 774–786.
[17] G. Fulgenzi, L. Graciotti, M. Faronato, M.V. Soldovieri, F. Miceli, S. Amoroso, L. Annunziato, A. Procopio, M. Taglialatela, Human neoplastic mesothelial cells express voltage-gated sodium channels involved in cell motility, Int. J. Biochem. Cell. Biol. 38 (2006) 1146–1159.
[18] D. Diaz, D.M. Delgadillo, E. Hernandez-Gallegos, M.E. Ramirez-Dominguez, L.M. Hinojosa, C.S. Ortiz, J. Berumen, J. Camacho, J.C. Gomora, Functional expression of voltage-gated sodium channels in primary cultures of human cervical cancer, J. Cell. Physiol. 210 (2007) 469–478.
[19] L.M. Coussens, Z. Werb, Inflammation and cancer, Nature 420 (2002) 860–867.
[20] J.W. Pollard, Tumour-educated macrophages promote tumour progression and metastasis, Nat. Rev. Cancer 4 (2004) 71–78.
[21] W.A. Catterall, From ionic currents to molecular mechanisms: the structure and function of voltage-gated sodium channels, Neuron 26 (2000) 13–25.
[22] W.F. Huang, S. Ouyang, S.Y. Li, Y.F. Lin, H. Ouyang, H. Zhang, C.J. Lu, Effect of quercetin on colon contractility and L-type Ca(2+) channels in colon smooth muscle of guinea-pig, Sheng Li Xue Bao 61 (2009) 567–576.
[23] L. Gillet, S. Roger, P. Besson, F. Lecaille, J. Gore, P. Bougnoux, G. Lalmanach, J.Y. Le Guennec, Voltage-gated sodium channel activity promotes cysteine cathepsin-dependent invasiveness and colony growth of human cancer cells, J. Biol. Chem. 284 (2009) 8680–8691.
[24] J.D. Malhotra, K. Kazen-Gillespie, M. Hortsch, L.L. Isom, Sodium channel beta subunits mediate homophilic cell adhesion and recruit ankyrin to points of cell-cell contact, J. Biol. Chem. 275 (2000) 11383–11388.
[25] L.L. Isom, The role of sodium channels in cell adhesion,, Front. Biosci. 7 (2002) 12–23.